ACS OMEGA

http://pubs.acs.org/journal/acsodf

Article

Structural Evolution and Microwave Dielectric Properties of $Ba_{1-x}Sr_xTi_4O_9$, $(0.0 \leq x \leq 0.06)$ Ceramics

Asad Ali,* Abid Zaman,* Sharah A. A. Aldulmani, Mujahid Abbas, Muhammad Mushtaq, Khalid Bashir, Mongi Amami, and Khaled Althubeiti

Cite This: https://doi.org/10.1021/acsomega.1c06212

Read Online

ACCESS | Metrics & More | Article Recommendations

ABSTRACT: The structural, microstructural, and microwave dielectric properties of $Ba_{1-x}Sr_xTi_4O_9$, $(0.0 \leq x \leq 0.06)$ ceramics samples synthesized by a conventional route were investigated. These structural, microstructural, and dielectric properties were recorded using X-ray diffraction (XRD), scanning electron microscopy (SEM), and Fourier transform infrared (FTIR) and impedance analyzer spectroscopies. Ti−O octahedral distortion was observed due to Sr^{2+} addition. The microwave dielectric properties were interrelated with various Sr^{2+} concentrations. Excellent microwave dielectric properties, i.e., high relative permittivity (ϵ_r = 71.50) and low dielectric loss ($\tan\delta$ = 0.0006), were obtained.

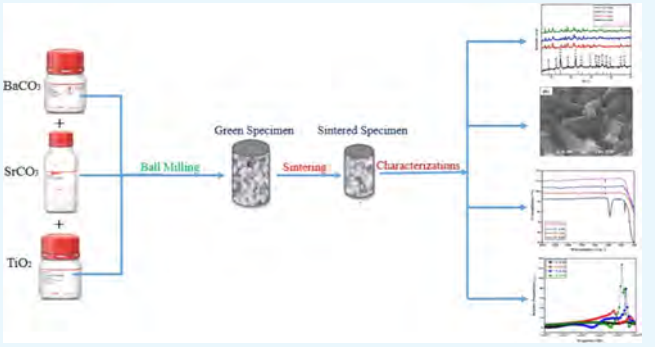

INTRODUCTION

Microwave dielectric devices are used in advanced technological systems such as radar, satellite receiver modules, and mobile telephones.[1] The dielectric material, which is used in telecommunication devices, is termed dielectric resonators (DRs). Dielectric resonators may be used to stabilize microwave oscillators and microwave filter frequencies. Barium titanate ($BaTiO_3$) and barium tetratitanate ($BaTi_4O_9$) are candidate materials for DRs in microwave telecommunication and satellite broadcasting.[2] Microwave DRs provide important advantages in terms of temperature stability, compactness, light weight, and comparatively low costs in the processing of high-dependence frequency devices.[3] The physical characteristics required for DRs are as follows.

(i) High relative permittivity (ε_r) to attain reduction of modules in the interpretation of $(1/\varepsilon_r^2)$, i.e., size dependence.
(ii) High quality factor ($Q \times f$) values to reduce tangent loss.
(iii) Small temperature coefficient of resonant frequency (τ_f) for stabilization of resonant frequency.

$BaTiO_3$, $BaTi_4O_9$, and doped $BaTi_4O_9$ compounds meet these basic requirements for the application of DRs; for example, ε_r = 39.11, $Q \times f$ = 10,700 GHz, and τ_f = + 14.2 ppm/°C.[4] However, it is essential for the synthesized dielectric ceramics to have the required microwave dielectric properties. Thus, the processing of single-phase ceramics is necessary to investigate different characterizations. The mixed oxide route involves a high calcination temperature during the reaction of $BaCO_3$ and TiO_2 (raw materials), and secondary phases may also be formed during the calcination process.[5−7] Additionally, the product may be contaminated with impurities from grinding media. Nagas et al. reported the effects of different additives on the phase and microwave dielectric properties of $BaTiO_3$ and $BaTi_4O_9$ ceramics.[8] The dielectric and structural properties of $BaTi_4O_9$ with different dopants have been studied in the microwave-frequency range.[9−13] The different types of additives, i.e., Sr in $BaTi_4O_9$ ceramics, result in multiple phases including $BaTi_4O_9$, $Ba_2Ti_9O_{20}$, and TiO_2.[11] Kolar et al.[14] and Negas et al.[15] determined the phases and investigated the microwave dielectric properties with a relatively lower frequency at 1 MHz. Several studies have been executed to improve the microwave dielectric properties of $BaTi_4O_9$ ceramics by doping different additives, i.e., Sr^{2+}, Ca^{2+}, Pb^{2+}, and Bi^{2+} ions for Ba^{2+} site-ion and Zr^{4+} and Sn^{4+} ions for Ti^{4+} site-ion.[16,17] Other synthesis routes such as sol gel and co-precipitation may also use to synthesize these products.[18,19]

Barium tetratitanate ($BaTi_4O_9$) ceramics is one of the well-known dielectric materials and has been studied by numerous researchers for use in dielectric resonators, thermistors, and electro-optic devices.[20] Due to its importance, in the present work, we studied the effect of Sr on phase, surface morphology,

Received: November 4, 2021
Accepted: December 22, 2021

and the dielectric properties of $BaTi_4O_9$ ceramics using a controlled mixed oxide solid-state processing route to prepare $(Ba_{1-x}Sr_x)Ti_4O_9$, $0.0 \leq x \leq 0.06$. These products have been analyzed using X-ray diffraction (XRD), scanning electron microscopy (SEM), and Fourier transform infrared (FTIR) spectroscopy. The dielectric properties of products were measured using impedance spectroscopy.

RESULTS AND DISCUSSION

Phase Analysis. The XRD pattern of $(Ba_{1-x}Sr_x)$ Ti_4O_9, $0.0 \leq x \leq 0.06$ sintered ceramics is shown in Figure 1. The XRD

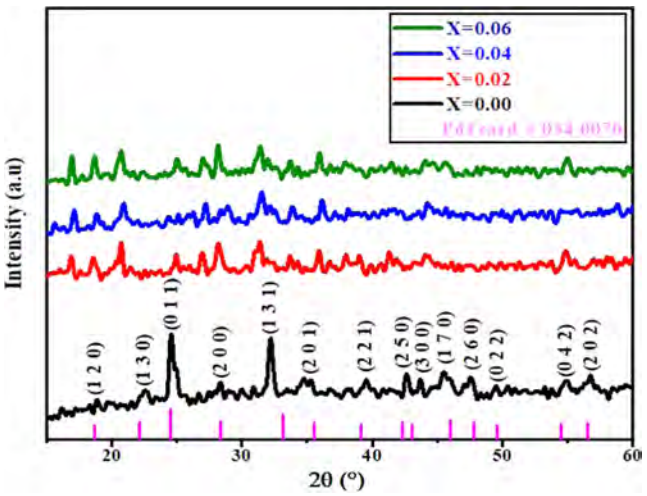

Figure 1. XRD pattern of $(Ba_{1-x}Sr_x)$ Ti_4O_9, $0.0 \leq x \leq 0.06$ ceramics.

studies revealed the formation of the orthorhombic ($Amm2$) structured base composition of barium tetratitanate ($BaTi_4O_9$), which matches with ICDD/PDF card # 034-0070. It is suggested that Sr^{2+} is incorporated in the lattice of the base composition to partially replace Ba^{2+} ions. A shift of XRD peaks was detected toward higher Bragg-angle (2θ) values with increasing Sr^{2+} content in $(Ba_{1-x}Sr_x)Ti_4O_9$. The shifting may be due to the substitution of relatively smaller cations of Sr^{2+} (R_{Sr} = 1.44 Å) for Ba^{2+}(R_{Ba} = 1.61 Å) following the Brags diffraction law ($2d \sin\theta = m\lambda$).[21,22] A peak at 32.4° emerges with an increase in Sr^{2+}, which is attributed to the transformation of the structure from orthorhombic ($Amm2$) at x = 0.0 to tetragonal ($I4/m$) at x = 0.02, 0.04 and then to cubic ($Pm3m$) at x = 0.06. The variation in lattice parameters with increasing Sr^{2+} content is attributed to the phase transition from orthorhombic to tetragonal and then to the cubic structure as listed in Table 1, while Table 2 represents the XRD data of the base composition ($BaTi_4O_9$).

The particle size and lattice strain of the $Ba_{1-x}Sr_xTi_4O_9$, $(0.00 \leq x \leq 0.06)$ sample were determined using the

Table 1. Structural Data of $(Ba_{1-x}Sr_x)$ Ti_4O_9, $0.0 \leq x \leq 0.06$ Ceramics

X	structure	space group	a (Å)	b (Å)	c (Å)
0.00	orthorhombic	$Amm2$	6.29400	14.5324	3.79720
0.02	tetragonal	$I4/m$	10.1434	10.1434	2.96795
0.04	tetragonal	$I4/m$	10.1434	10.1434	2.96795
0.06	cubic	$Pm3m$	3.89800	3.89800	3.89800

Table 2. X-ray Diffraction Data for the Base Composition ($BaTi_4O_9$) at λ = 0.154 nm

$2\theta_{exp}$	$2\theta_{calc}$	I_{exp}	h	k	l	d_{exp}	d_{calc}
18.85	18.63	105.82	1	2	0	4.70211	4.75713
22.45	23.14	140.18	1	3	0	3.95557	3.83916
24.55	24.20	366.33	0	1	1	3.62176	3.67334
28.20	28.34	163.72	2	0	0	3.16072	3.14543
32.30	33.15	303.62	1	3	1	2.76826	2.69921
35.30	36.08	184.69	2	0	1	2.53956	2.48643
38.39	37.61	174.98	2	1	1	2.34196	2.38872
42.55	42.32	195.27	2	5	0	2.12212	2.13312
43.60	43.06	168.88	3	0	0	2.07342	2.09816
45.65	45.99	206.25	1	7	0	1.98496	1.97107
47.75	47.30	179.09	2	6	0	1.90244	1.91949
49.60	49.59	156.41	0	2	2	1.83573	1.83607
54.80	54.51	174.53	0	4	2	1.67319	1.68141
56.85	56.56	199.23	2	0	2	1.61762	1.62522

Williamson–Hall (W–H) technique from the broadening of the XRD peaks.[23]

$$\beta \cos\theta = \frac{k\lambda}{D} + 4\varepsilon \sin\theta \quad (1)$$

The equation represents a straight line, where ε is the gradient (slope) of the line and $k\lambda/D$ is the y-intercept.

Consider the standard equation of a straight line,

$$y = mx + c \quad (2)$$

Now, we plot $4 \sin\theta$ on the x-axis and $\beta \cos\theta$ on the y-axis.

The value of the strain ($\varepsilon_{W\text{-}H}$) is given by the value of "m", which represents the gradient (slope) of the line, and the crystallite size can be calculated from the y-intercept $k\lambda/D$.

Figure 2a–d shows Williamson–Hall (W–H) plots for $Ba_{1-x}Sr_xTi_4O_9$, $(0.00 \leq x \leq 0.06)$ ceramics. The W–H is used for deconvoluting shapes (crystalline shapes) and strain that contributes to X-ray line broadening because Scherrer's formula does not take into account the strain contribution.

Therefore, the average crystallite size, dislocation density, and strain of W–H lie in the 2.9449–11.6128 Å, 0.74152×10^{-6}–271.667×10^{-6}, and 1.1949×10^{-3}–22.871×10^{-3} ranges for $Ba_{1-x}Sr_xTi_4O_9$, $(0.00 \leq x \leq 0.06)$ ceramics, respectively, as shown in Table 3.

Mathematically, the dislocation density (δ) was calculated using the equation[24]

$$\delta = \frac{1}{D^2} \quad (3)$$

Dislocation strongly influences many other properties of materials. As the dopant element perfectly replaces the host ions in the crystal lattice, it improves the crystal structure and produces very small crystal defects that can be negligible.

The lattice strain (η) was calculated through the equation[25,26]

$$\eta = \frac{\beta \cos\theta}{4} \quad (4)$$

In Table 3, the deviation in the calculated lattice strain and crystallite sizes of all prepared $Ba_{1-x}Sr_xTi_4O_9$, $(0.00 \leq x \leq 0.06)$ ceramics samples with compositions is shown. When the concentration of the dopant element is increased, the microstrain decreases due to the size of the dopant element being greater than the host ions, as shown in Table 3.

https://doi.org/10.1021/acsomega.1c06212
ACS Omega XXXX, XXX, XXX–XXX

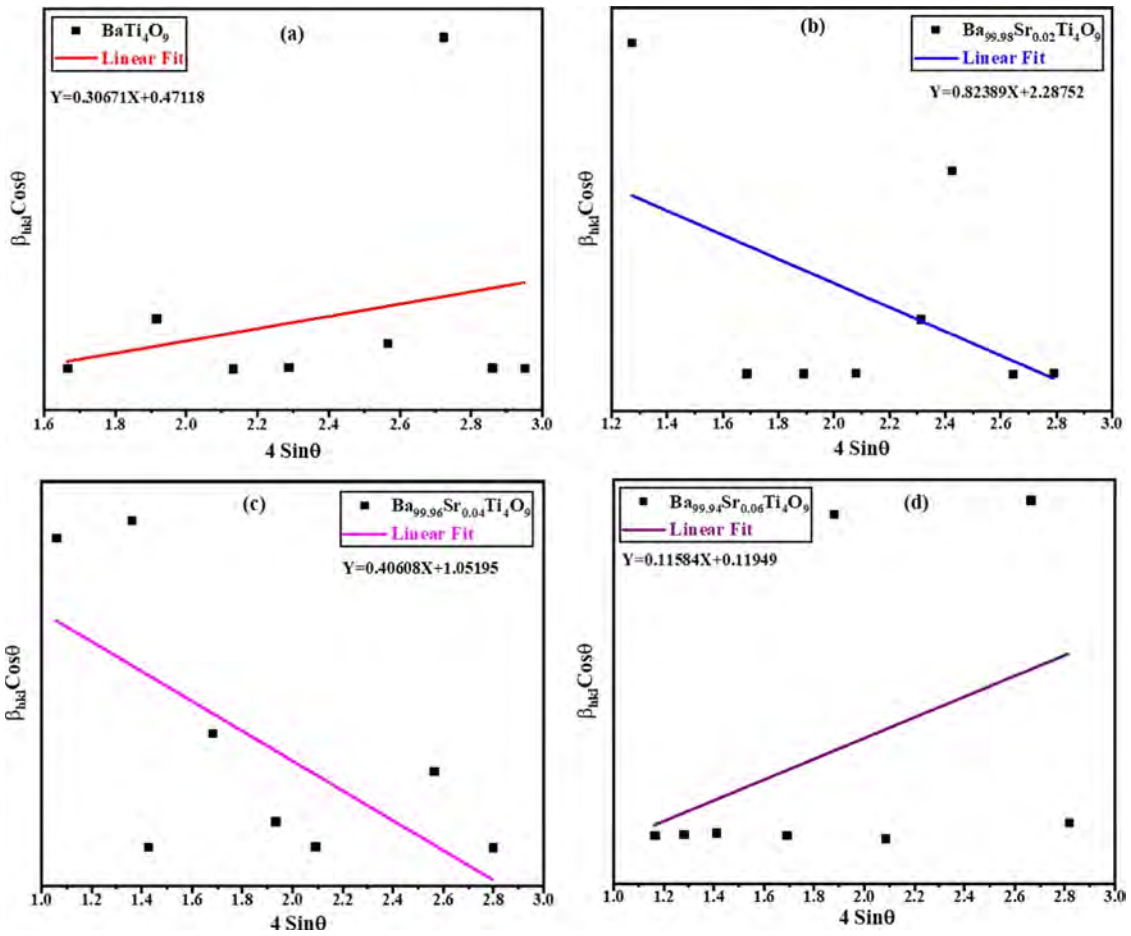

Figure 2. Williamson–Hall plot of $Ba_{1-x}Sr_xTi_4O_9$ with Sr content (a) $X = 0.00$, (b) $X = 0.02$, (c) $X = 0.04$, and (d) $X = 0.06$.

Table 3. Williamson–Hall (W–H) Calculated Crystallite Size ($D_{W\text{-}H}$), Dislocation Density ($\delta_{W\text{-}H}$), and Strain ($\eta_{W\text{-}H}$) $Ba_{1-x}Sr_xTi_4O_9$, ($0.00 \leq x \leq 0.06$)

composition	$D_{W\text{-}H}$ (nm)	$\delta_{W\text{-}H}$ ($\times 10^{-6}$ nm^{-2})	$\eta_{W\text{-}H}$ ($\times 10^{-3}$)
0.00	0.29449	11.5301	4.7118
0.02	0.06067	271.667	22.871
0.04	0.13191	57.4710	10.519
0.06	1.16128	0.74152	1.1949

Microstructural Analysis. The SEM images of $(Ba_{1-x}Sr_x)Ti_4O_9$, $0.0 \leq x \leq 0.06$ ceramics sintered at 1300 °C in air for 2 h, polished, and thermally etched are shown in Figure 3. The SEM images indicated a dense microstructure with no obvious pores and grains, exhibiting elongated platelike morphologies for the base composition ($x = 0.00$), which is consistent with previous reports for the orthorhombic-structured BaTi4O9.[27,28] The grain morphologies were observed to change from elongated to rectangular with an increase in the Sr^{2+} content. The grain size for $x = 0.00$ is about 10×1 μm^2 and decreases with increasing Sr^{2+} content. The variation of relative densities (ρ_r) with increasing Sr^{2+} content is shown in Table 4. The maximum theoretical density achieved is 4.94 g/cm^3 as listed in Table 3. The increase in density may affect the value of the dielectric constant.[11]

FTIR Spectroscopy. The FTIR spectra of $(Ba_{1-x}Sr_x)Ti_4O_9$, $0.0 \leq x \leq 0.06$ ceramics have been studied as shown in Figure 4. Very strong absorption peaks appear near 800 and 1400 cm^{-1} at $x = 0.00$, while minor peaks are also observed at $x > 0.00$ near 1600 cm^{-1}. These peaks revealed the Ti–O octahedral vibrations according to previous studies on titanates.[29] Due to the addition of Sr^{2+}, the concentration in the solid solution of BaT_4O_9 ceramics is been shifted to higher wavenumbers. Sun et al. reported that only one oxygen vacancy can be used to replace Ba^{2+} ion, while the remaining three oxygen vacancies were used to replace the produced Ti^{4+} ion using respective additives.[30] Therefore, Ti–O octahedra are easily distorted or damaged in this way. Some vibrational modes were observed in the FTIR spectrum. Therefore, relative studies of the FTIR spectrum further support the development of redispersibility of polycrystalline BaT_4O_9 ceramic dielectrics.

Microwave Dielectric Properties. The microwave dielectric properties of $(Ba_{1-x}Sr_x)Ti_4O_9$, $0.0 \leq x \leq 0.06$ ceramics have also been investigated, as shown in Figure 5. The dielectric constant (ε_r) varies from 21.9 3 to 71.50, while the variation in dielectric loss ($\tan\delta$) with Sr^{2+} is shown in Table 4. The maximum value of $\tan\delta$ (0.0006) was observed. The frequency-dependent quality factor (Q) is a dimensionless physical quantity, and quantitatively, it is expressed in terms of $Q \times f$.[31−35]

The variations of $\tan(\delta)$ with frequency (f) for various Sr^{2+} contents in $(Ba_{1-x}Sr_x)Ti_4O_9$, $0.0 \leq x \leq 0.06$ are shown in Figure 6. The orientation polarization decreases with increasing frequency and results in an increase in dielectric loss, which may be attributed to the time lag between flipping dipoles and the applied electric field.[1,36−38] Microwave

https://doi.org/10.1021/acsomega.1c06212
ACS Omega XXXX, XXX, XXX−XXX

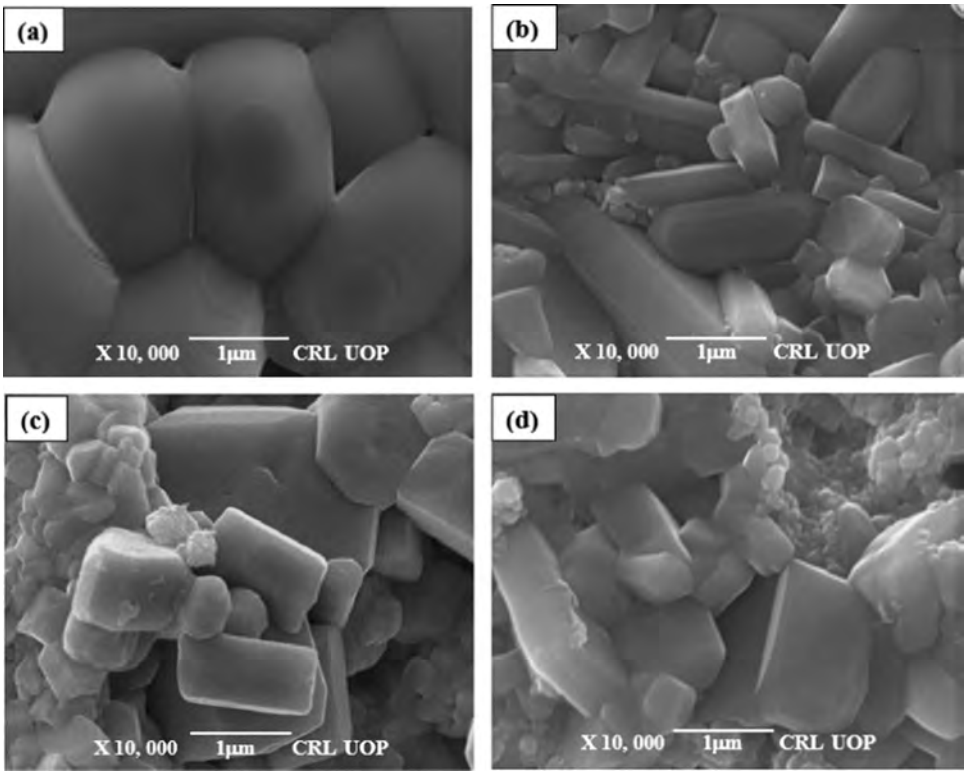

Figure 3. SEM images of $(Ba_{1-x}Sr_x)$ Ti_4O_9, $0 \leq x \leq 0.06$ ceramics polished and thermally etched: (a) $x = 0.00$, (b) $x = 0.02$, (c) $x = 0.04$, and (d) $x = 0.06$ indicating a decrease in grain size and change in grain morphologies with an increase in Sr^{2+} content.

Table 4. Density Parameters and Dielectric Properties of $(Ba_{1-x}Sr_x)$ Ti_4O_9, $0.0 \leq x \leq 0.06$ Ceramics[a]

X	ρ_a (g/cm^3)	ρ_t (g/cm^3)	ρ_r (%)	tan δ	ε_r
0.00	4.26	4.402	96.77	0.0008	21.93
0.02	4.40	4.840	90.90	0.0006	47.84
0.04	4.40	4.940	89.07	0.0043	71.50
0.06	4.07	4.540	89.64	0.0044	52.50

[a]Note: ρ_a = apparent density, ρ_t = theoretical density, and ρ_r = relative density.

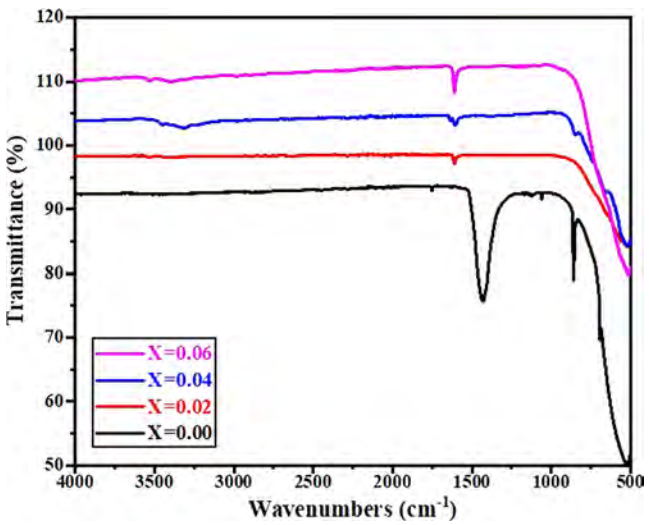

Figure 4. FTIR spectra of $(Ba_{1-x}Sr_x)$ Ti_4O_9, $0.0 \leq x \leq 0.06$ ceramics.

dielectric material is usually characterized by high relative permittivity and a low tangent loss. The theoretical justification

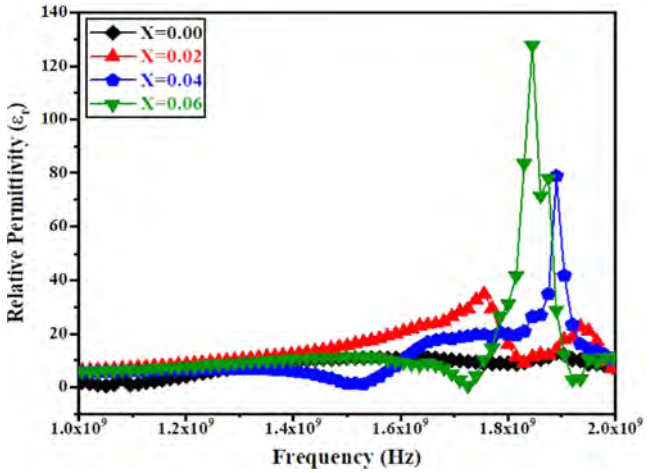

Figure 5. Variation of ε_r with the frequency of $(Ba_{1-x}Sr_x)$ Ti_4O_9, $0.0 \leq x \leq 0.06$ ceramic.

is very important for this case in which ionic crystals with an optical mode of vibrations resonate at a frequency of (10^{13} Hz). In the frequency range from approximately 10^9 to 10^{11} Hz, the dielectric dispersion theory shows the contribution to polarization from the ionic displacement to be nearly constant and the loss to increase with frequency.[39]

CONCLUSIONS

The structural, microstructural, and microwave dielectric properties of $(Ba_{1-x}Sr_x)Ti_4O_9$, $0.0 \leq x \leq 0.06$ sintered ceramics were investigated via a solid-state route. It is found that the dielectric constant (ε_r) and dielectric loss (tan δ) values improved with Sr^{2+} content. The $(Ba_{0.98}Sr_{0.02})Ti_4O_9$

https://doi.org/10.1021/acsomega.1c06212
ACS Omega XXXX, XXX, XXX−XXX

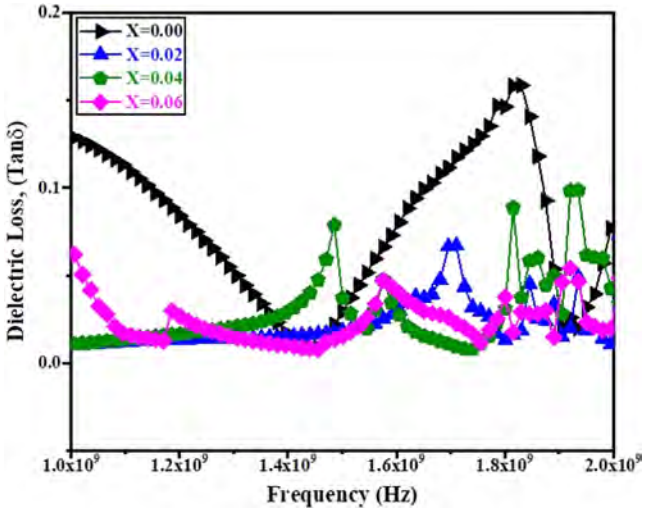

Figure 6. Variation of tan δ with frequency (f) for various Sr^{2+} contents in $(Ba_{1-x}Sr_x)$ Ti_4O_9, $0.0 \leq x \leq 0.06$ ceramics.

ceramics was found to have the best ε_r and tan δ values. The microwave dielectric properties of $(Ba_{0.98}Sr_{0.02})Ti_4O_9$ ceramics intensely depend upon density. Outstanding microwave dielectric properties of $\varepsilon_r \sim 47.84$ and tan $\delta \sim 0.0006$ were obtained for $(Ba_{0.98}Sr_{0.02})Ti_4O_9$ ceramics sintered at 1300 °C for 2 h. We obtained excellent microwave dielectric properties in this study for the application of microwave wireless communication systems.

EXPERIMENTAL PROCEDURE

$BaCO_3$ (purity 99.0%, Chemdad, China), $SrCO_3$ (purity 99.5%, ABSCO, U.K.), and TiO_2 (purity 99.9%, Sigma) were chosen as raw starting materials to prepare $(Ba_{1-x}Sr_x)Ti_4O_9$, $0.0 \leq x \leq 0.06$ ceramics material for microwave dielectric devices. The raw materials, i.e., $BaCO_3$, $SrCO_3$, and TiO_2, were thoroughly mixed according to the $(Ba_{1-x}Sr_x)$ Ti_4O_9, $0 \leq x \leq 0.06$ stoichiometric ratios, where the mole ratio of A site-ion and B site-ion was 1:4. Distilled water was added to the weighed raw material powder in a polyethylene jar container along with 5 mm diameter zirconia balls and then milled by horizontal ball milling for 24 h. The mixture powders were dried at 100 °C for 24 h in an air atmosphere, and after drying, the reactant mixture was loaded in an alumina crucible and calcined at 1000 °C for 3 h in air at 10 °C/min in a heating/cooling rate. After calcination, the product powder was ground and then pressed into green body discs (5 mm thickness and 10 mm diameter) under a pressure of 80 MPa using a manual pellet press (CARVER). The pellet samples were sintered at 1300 °C for 2 h in air with a heating/cooling rate of 10 °C/min. The crystalline phases of the calcined $(Ba_{1-x}Sr_x)$ Ti_4O_9, $0.0 \leq x \leq 0.06$ ceramics samples were identified using X-ray diffraction (XRD) (JDX-3532, JEOL, Japan) with a Cu Kα (λ = 0.15406 nm) radiation source operated at 40 mA and 40 kV in a wide range of Braggs angle 2θ ($20° < 2\theta < 80°$) at a scanning rate of 2°/min. The surface morphology information was obtained using SEM (JSM-5910, JEOL Japan), while the microwave dielectric properties of the sintered samples were measured at microwave frequencies using impedance spectroscopy (Agilent 4287A).

AUTHOR INFORMATION

Corresponding Authors

Asad Ali − *Department of Physics, Government Postgraduate College Nowshera, Nowshera 24100 KP, Pakistan*; Email: kasadiiui@gmail.com

Abid Zaman − *Department of Physics, Riphah International University, Islamabad 44000, Pakistan*; orcid.org/0000-0001-9527-479X; Email: zaman.abid87@gmail.com

Authors

Sharah A. A. Aldulmani − *Department of Chemistry, King Khalid University, Abha 62529, Saudi Arabia*

Mujahid Abbas − *Faculty of Materials and Manufacturing, Beijing University of Technology, Beijing 100124, China*

Muhammad Mushtaq − *Faculty of Materials and Manufacturing, Beijing University of Technology, Beijing 100124, China*

Khalid Bashir − *Department of Physics, Riphah International University, Islamabad 44000, Pakistan*

Mongi Amami − *Department of Chemistry College of Sciences, King Khalid University, Abha 62529, Saudi Arabia; Laboratoire des matériaux et de l'environnement pour le développement durable LR18ES10, 1006 Tunis, Tunisia*

Khaled Althubeiti − *Department of Chemistry, College of Science, Taif University, Taif 21944, Saudi Arabia*

Complete contact information is available at: https://pubs.acs.org/10.1021/acsomega.1c06212

Author Contributions

This work was carried out in collaboration with all authors. A.A. prepared samples and wrote the original draft of the manuscript. A.Z. performed the final writing review, corrections, and editing. M.A. helped in methodology and measurements. S.A.A. and M.M. prepared content analysis and graphical arrangements. K.B. helped with software and validation. K.A. and M.A. helped with formal analysis and provided funding acquisition. All authors have read and approved the final manuscript.

Notes

The authors declare no competing financial interest.

ACKNOWLEDGMENTS

Taif University Researchers Supporting Project number (TURSP-2020/241), Taif University, Taif, Saudi Arabia. The authors acknowledge to extend their appreciation to the Deanship of Scientific Research at King Khalid University, Saudi Arabia, for funding this work through the Research Groups Program under grant number R.G.P.1: 43/42.

REFERENCES

(1) Sebastian, M. T. *Dielectric Materials for Wireless Communication*; Elsevier: Oxford, UK, 2010.

(2) Cava, R. J. Dielectric materials for applications in microwave communications. *J. Mater. Chem.* **2001**, *11*, 54−62.

(3) Freer, R.; Azough, F. Microstructural engineering of microwave dielectric ceramics. *J. Eur. Ceram. Soc.* **2008**, *28*, 1433−1441.

(4) Rase, D. E.; Roy, R. Phase equilibria in the system BaO−TiO2. *J. Am. Ceram. Soc.* **1955**, *38*, 102−113.

(5) Ali, A.; Uddin, S.; Iqbal, Z.; Lal, M.; Zaman, A. Structural, optical and microwave dielectric properties of barium tetra titanate (BaTi4O9) ceramics. *J. Optoelectron. Adv. Mater.* **2021**, *23*, 48−52.

https://doi.org/10.1021/acsomega.1c06212
ACS Omega XXXX, XXX, XXX−XXX

(6) Phule, P. P.; Risbud, S. H. Low-temperature synthesis and processing of electronic materials in theBaO-TiO2 system. *J. Mater. Sci.* **1990**, *25*, 1169−1183.
(7) Negas, T.; Yeager, G.; Bell, S.; Coats, N.; Minis, I. BaTi4O9/Ba2Ti9O20-based ceramics resurrected for modern microwave applications. *Am. Ceram. Soc. Bull.* **1993**, *72*, 80−89.
(8) Mhaisalkar, S. G.; Readey, D. W.; Akbar, S. A.; Dutta, P. K.; Sumner, M. J.; Rokhlin, R. Infrared reflectance spectra of doped BaTi4O9. *J. Solid State Chem.* **1991**, *95*, 275−282.
(9) Nishigaki, S.; Yano, S.; Kato, H.; Hirai, T.; Nonomura, T. BaO-TiO2-WO3 Microwave Ceramics and Crystalline BaWO4. *J. Am. Ceram. Soc.* **1988**, *71*, C−11.
(10) Ern, V.; Newnham, R. E. Effect of WO3 on dielectric properties of BaTiO3 ceramics. *J. Am. Ceram. Soc.* **1961**, *44*, 199.
(11) Mhaisalkar, S. G.; Lee, W. E.; Readey, D. W. Processing and characterization of BaTi4O9. *J. Am. Ceram. Soc.* **1989**, *72*, 2154−2158.
(12) Kolar, D.; Gaberscek, S.; Volavsek, B.; Parker, H. S.; Roth, R. S. Synthesis and crystal chemistry of BaNd2Ti3O10, BaNd2Ti5O14, and Nd4Ti9O24. *J. Solid State Chem.* **1981**, *38*, 158−164.
(13) Davies, P. K.; Roth, R. S.; Clevinger, M. A. editors. *Chemistry of Electronic Ceramic Materials*; CRC Press, 1991.
(14) Pei, J.; Yue, Z.; Zhao, F.; Gui, Z.; Li, L. Effects of Silver Doping on the Sol−Gel-Derived Ba4 (Nd0. 7Sm0. 3) 9.33 Ti18O54 Microwave Dielectric Ceramics. *J. Am. Ceram. Soc.* **2007**, *90*, 3131−3137.
(15) Qin, N.; Liu, X. Q.; Chen, X. M. Thermal Expansion and High-Temperature Phase Transition of Ba6− 3xLn8+ 2xTi18O54 (Ln= La, Nd, and Sm) Ceramics. *J. Am. Ceram. Soc.* **2007**, *90*, 2912−2917.
(16) Okawa, T.; Imaeda, M.; Ohsato, H. Microwave dielectric properties of Bi-added Ba4Nd9+ 1/3Ti18O54 solid solutions. *Jpn. J. Appl. Phys.* **2000**, *39*, 5645−5649.
(17) Wu, Y. J.; Chen, X. M. Bismuth/samarium cosubstituted Ba6−3xNd8+ 2xTi18O54 microwave dielectric ceramics. *J. Am. Ceram. Soc.* **2000**, *83*, 1837−1839.
(18) Belous, A. G.; Ovchar, O. V.; Valant, M.; Suvorov, D.; Kolar, D. The effect of partial isovalent substitution in the A-sublattice on MW properties of materials based on Ba6−xLn8+ 2x/3Ti18O54 solid solutions. *J. Eur. Ceram. Soc.* **2001**, *21*, 2723−2730.
(19) Avinash, M.; Muralidharan, M.; Selvakumar, S.; Hussain, S.; Sivaji, K. Induced ferromagnetism and enhanced optical behaviour in indium-doped barium stannate system. *J. Mater. Sci.: Mater. Electron* **2020**, *31*, 3375−3386.
(20) Chen, X. M.; Li, Y. A-and B Site Cosubstituted Ba6− 3xSm8+ 2xTi18O54Microwave Dielectric Ceramics. *J. Am. Ceram. Soc.* **2002**, *85*, 579−584.
(21) Tong, X. D.; Sun, Y. Nd−Fe−B alloy-densified agarose gel for expanded bed adsorption of proteins. *J. Chromatogr. A.* **2002**, *943*, 63−75.
(22) Wah Chan, L.; Liu, X.; Heng, P. W. Liquid phase coating to produce controlled-release alginate microspheres. *J. Microencapsulation.* **2005**, *22*, 891−900.
(23) Avinash, M.; Muralidharan, M.; Sivaji, K. Structural, optical and magnetic behaviour of Cr doped BaSnO3 perovskite nanostructures. *Phys. B* **2019**, *570*, 157−65.
(24) Zaman, A.; Uddin, S.; Mehboob, N.; Ali, A. Structural investigation and improvement of microwave dielectric properties in Ca (HfxTi1-x) O3 ceramics. *Phys. Scr.* **2020**, *96*, No. 025701.
(25) Zaman, A.; Uddin, S.; Mehboob, N.; Ali, A.; Ahmad, A.; Bashir, K. Effect of Zr4+ on the structural and microwave dielectric properties of CaTiO3 ceramics. *Ferroelectrics* **2021**, *577*, 143−152.
(26) Abbas, M.; Ullah, R.; Ullah, K.; Sultana, F.; Mahmood, A.; Mateen, A.; Zhang, Y.; Ali, A.; Althubeiti, K.; Mushtaq, M.; Zaman, A. Structural, optical, electrical and dielectric properties of (Sr1-xMgx)(Sn0. 5Ti0. 5) O3 (X= 0.00, 0.25, 0.50, 0.75) ceramics via solid state route. *Ceram. Int.* **2021**, *47*, 30129−30136.
(27) Wang, S. F.; Hsu, Y. F.; Wang, Y. R.; Cheng, L. T.; Hsu, Y. C.; Chu, J. P.; Huang, C. Y. Densification, microstructural evolution and dielectric properties of Ba6− 3x (Sm1− yNdy) 8+ 2xTi18O54 microwave ceramics. *J. Am. Ceram. Soc.* **2006**, *26*, 1629−1635.
(28) Qin, N.; Liu, X. Q.; Chen, X. M. Phase Transition in Ba6− 3x (Sm1− yLay) 6+ 2xTi18O54 (x= 0.5) Ceramics. *J. Am. Ceram. Soc.* **2006**, *89*, 2796−2803.
(29) Perry, C. H.; Khanna, B. N.; Rupprecht, G. Infrared studies of perovskite titanates. *Phys. Rev.* **1964**, *135*, No. A408.
(30) Sun, D.; Jin, X.; Liu, H.; Zhu, J.; Zhu, Y.; Zhu, Y. Investigation on FTIR spectrum of barium titanate ceramics doped with alkali ions. *Ferroelectrics* **2007**, *355*, 145−148.
(31) Wu, J. M.; Chang, M. C.; Yao, P. C. Reaction Sequence and Effects of Calcination and Sintering on Microwave Properties of (Ba, Sr) O-Sm2O3-TiO2 Ceramics. *J. Am. Ceram. Soc.* **1990**, *73*, 1599−1605.
(32) Wang, S. F.; Yang, T. C.; Chiang, C. C.; Tsai, S. H. Effects of additives on the phase formation and microstructural evolution of Ba2Ti9O20 microwave ceramic. *Ceram. Int.* **2003**, *29*, 77−81.
(33) Wu, J. M.; Wang, H. W. Factors affecting the formation of Ba2Ti9O20. *J. Am. Ceram. Soc.* **1988**, *71*, 869−875.
(34) Purohit, R. D.; Tyagi, A. K. Synthesis of monophasic Ba2Ti9O20 through gel combustion. *J. Mater. Chem.* **2002**, *12*, 1218−1221.
(35) Shannon, R. D. Revised effective ionic radii and systematic studies of interatomic distances in halides and chalcogenides. *Acta Crystallogr., Sect. A: Cryst. Phys., Diffr., Theor. Gen. Crystallogr.* **1976**, *32*, 751−767.
(36) Zaman, A.; Uddin, S.; Mehboob, N. Synthesis and Microwave Dielectric Characterization of Ca1-xSrxTiO3, Low-Loss Ceramics. *Iran J. Sci. Technol., Trans. A: Sci.* **2021**, *45*, 367−371.
(37) Ma, H.; Zhang, W.; Kong, X.; Uemura, S.; Kusunose, T.; Feng, Q. BaTi4O9 mesocrystal: Topochemical synthesis, fabrication of ceramics, and relaxor ferroelectric behavior. *J. Alloys Compd.* **2019**, *777*, 335−343.
(38) Luo, T.; He, L.; Yang, H.; Yu, H. Phase evolution and microwave dielectric properties of BaTi4O9 ceramics prepared by reaction sintering method. *Int. J. Appl. Ceram. Technol.* **2019**, *16*, 146−151.
(39) Sebastian, M. T.; Ubic, R.; Jantunen, H. Low-loss dielectric ceramic materials and their properties. *Int. Mater. Rev.* **2015**, *60*, 392−412.

https://doi.org/10.1021/acsomega.1c06212
ACS Omega XXXX, XXX, XXX−XXX